BUCKLING OF FUNCTIONALLY GRADED PLATES WITH VARYING IN-PLANE LOADING

Submitted by
Ramba Balamurali Krishna
(213CE2072)

M. Tech
In
Structural Engineering

under the guidance of
Prof. A. V. Asha
NIT Rourkela

Department of Civil Engineering
National Institute of Technology Rourkela
Orissa -769008, India

DEPARTMENT OF CIVIL ENGINEERING

NATIONAL INSTITUTE OF TECHNOLOGY, ROURKELA

ODISHA, INDIA

CERTIFICATE

This is to certify that the thesis entitled "**BUCKLING OF THE FUNCTIONALLY GRADED PLATE WITH VARYING IN PLANE LOADING**", submitted by **MR. RAMBA BALAMURALI KRISHNA** bearing **Roll no. 213CE2072** in partial fulfillment of the requirements for the award of ***Master of Technology*** in the Department of Civil Engineering, National Institute of Technology, Rourkela is an authentic work carried out by him under my supervision and guidance.

To the best of my knowledge, the matter embodied in the thesis has not been submitted to any other university/institute for the award of any Degree or Diploma.

Place: Rourkela **Prof. A. V. ASHA**

Date: Civil Engineering Department

National Institute of Technology, Rourkela

A C K N O W L E D G E M E N T

It gives me immense pleasure to express my deep sense of gratitude to my supervisor **Prof. A V Asha** for her valuable guidance, motivation, constant inspiration and above all for her ever co-operating attitude that enabled me to bring up this thesis to the present form.

I express my sincere thanks to the Director, Prof. S.K.Sarangi, National Institute of Technology, Rourkela for motivating me in this endeavor and providing me the necessary facilities for this study.
I am extremely thankful to **Prof. S.K. Sahu**, Head, and Department of Civil Engineering for providing all kinds of possible help and advice during the course of this work.

I am greatly thankful to all the staff members of the department and all my well-wishers, class mates and friends for their inspiration and help.

Place: Rourkela

Date**:**

RAMBA BALAMURALI KRISHNA

M. Tech., Roll No: 213CE2072
Specialization: Structural Engineering

Department of Civil Engineering
National Institute of Technology, Rourkela

ABSTRACT

Functionally graded materials are materials with a spatial variation of material properties. The FGM plates have significant applications in turbine blades, helicopter blades, compressor blades, aircraft or marine propellers. Many of these plates are subjected to in-plane load due to fluid or air pressure. Hence it is necessary to study their behavior under different types of loads. Study of buckling of functionally graded material (FGM) plates with different boundary conditions under varying in-plane load is therefore an important study. In these days, FGM have many engineering applications because of their high stiffness and strength.

The analysis is completed utilizing ANSYS programming. In ANSYS, the SHELL 281 component with six degrees of freedom per node is utilized. Twelve by twelve mesh and twelve layers were chosen for the analysis as per the results obtained in convergence study. Buckling of FGM plates with different in plane loading are studied. The effect of different parameters like width to thickness proportion, aspect ratio, gradient index and boundary conditions on the buckling load of FGM plates with varying in-plane load were studied.

It is observed that for all edges simply supported, all edges clamped and cantilever plates, with increasing aspect ratio and gradient index, the non-dimensional buckling load decreases. With increasing the side width (b/h) ratio, the non-dimensional buckling load increases.

Keywords: Functionally graded material, varying in-plane load, buckling

CONTENTS

List of figures

List of tables

Nomenclature

a ,b	Panel dimension of the FGM plate
a/ b	aspect ratio of the twisted plate
$A_{ij,}$ B_{ij} , Dij and S_{ij}	Extensional, bending-stretching coupling, Bending and transverse shear stiffnesses
b/h	width to thickness ratio of the twisted plate
[B]	Strain-displacement matrix for the element
[D]	stress-strain matrix
dx, dy	element length in x and y-direction
dV	volume of the element
E_{11},E_{22}	Moduli of elasticity in longitudinal and Transverse directions
$G_{12,}G_{13,}G_{23}$	Shear modulii
k	shear correction factor
K_e	global elastic stiffness matrix
K_E	element bending stiffness matrix with Shear deformation of the panel

K_x , K_y , K_{xy}	Bending strains
M_x,M_y,M_{xy}	Moment resultants of the twisted panel
n	number of layers of the FGM plate
[N]	Shape function matrix
N_i	Shape functions
N_{cr}	Critical load
η	load parameter
N_x , N_y , N_{xy}	In-plane stress resultants of the twisted plate
N^0_x, N^0_y	External loading in the X and Y directions respectively
[P]	Mass density parameters
q	Vector of degrees of freedom
Q_x, Q_y	Shearing force
R_X, R_y, R_{Xy}	Radii of curvature of shell in x and y directions and radius of twist
u,v,w	displacement components in the x, y, z directions at any point
u_0, v_0, w_0	Displacement components in the x, y, z directions at the mid surface
w	out of plane displacement
X,Y,Z	global coordinate axis system

CHAPTER 1

INTRODUCTION

1.1 INTRODUCTION

Functionally graded materials are materials with a spatial variation of material properties. The volume fractions of two or more materials may be varied continuously either only along the thickness direction or as a function of the in-plane dimensions. FGMs are usually made from a mixture of metals and ceramic. In this thesis, we consider plates in which the material properties change continuously through the thickness.

These FGM plates are used in various engineering applications and they are often subjected to dynamic loading. FGMs are used by the engineering community mainly in nuclear plants and spacecraft of high temperature applications as FGMs can withstand high temperatures. Presently they are also used in structural walls, body coatings for cars, and in sports products. In the FGMs, interface problems are eliminated by changing the volume fraction of constituent materials smoothly and continuously from surface to surface.

Many studies have been conducted on free vibration analysis and dynamic response of the functionally graded material plates subject to dynamic loading. Functionally graded materials, due to their mechanical and thermal merits compared to singly composed materials, have been widely used for a variety of engineering applications. FGMs have different applications especially for aerospace, automobiles, industries and engineering structures and electronics.

CHAPTER 2
LITERATURE REVIEW

2.1 LITERATURE REVIEW

Plenty of studies for vibration, thermal stress and thermal bending of the functionally graded plates are available in the literature.

Praveen and Reddy (1998) investigated the nonlinear static and dynamic response of functionally graded ceramic–metal plates in a steady temperature field. The plate was subjected to dynamic transverse loads. They used the finite element method (FEM) based on the first-order shear deformation plate theory (FSDPT).

Reddy (2000) investigated functionally graded plates, based on the third-order shear deformation plate theory. Numerical results of the linear third-order theory and non-linear first-order theory were presented to show the effect of the material distribution on the deflections and stresses.

A semi-analytical solution for the nonlinear vibration of laminated FGM plates with geometric imperfections was presented by Yang *et al.* (2001). They showed that the vibration frequencies are very much dependent on the vibration amplitude and the imperfection mode.

Chung and Chi (2001) studied functionally graded material (FGM) plate of medium thickness subjected to transverse stacking.

Javaheri and Eslami (2002) investigated rectangular functionally graded plates (FGPs) using the variational methodology.

The vibration characteristics and transient response of shear-deformable functionally graded plates and panels in thermal environments was studied by Yang and Shen (2002, 2003). They considered material properties to be temperature-dependent and the effect of temperature rise on the dynamic response was reported.

Lanhe (2004) studied stability of a rectangular plate made of functionally graded material (FGM) under loads.

Kang and Leissa (2005) formulated an exact solution for the buckling analysis of rectangular plates having two opposite edges simply supported. These edges were subjected to linearly varying normal stresses.

Abrate (2006) presented free vibration, buckling, and static deflections of functionally graded plates. He showed that natural frequencies of the functionally graded plates were proportional to the homogeneous isotropic plates.

Ebrahimi and Rastgo (2008) investigated the free vibration of smart FGM plates. They studied FGM plates integrated with two uniformly distributed actuator layers made of piezoelectric (PZT4) material on the top and bottom surfaces of the circular FG plate based on the classical plate theory (CPT).

Saha and Maiti (2012) studied the buckling behavior of simply supported FGM plates under constant and linearly varying in-plane loads. They observed that the behavior of FGM plates was quite similar to that of isotropic plates. They also found that the ratio of the buckling load of FGM plates to that of the isotropic plate was independent of loading parameter, aspect ratio, etc.

A higher order shear deformation theory was used by Reddy *et al*. (2012) to study the buckling behavior of simply supported FGM plates without considering the zero transverse shear stresses at the top and bottom of the plate. The effect of various parameters on the critical buckling load was investigated.

Alinia *et al.* (2012) analysed inelastic clasping and post clasping conduct of stocky plates under joined shear and in-plane twisting hassles. They compared the results with slim plates.

Wattanasakulpong *et al.* (2012) investigated the free vibration of functionally graded beams with general elastic end constraints by DTM. The boundary conditions were arbitrary, and various types of elastically end constraints were analyzed.

Hadi *et al.* (2013) presented an elastic analysis of transverse loading acting on the functionally graded beam. They determined the stresses and strains on FG beam by using energy method, and also used power law for varying thickness. This gave the exact solution for stresses and displacements.

2.2 OBJECTIVE OF PRESENT STUDY

FGM has many applications in engineering and aerospace structures. The idea arose out of making a composite material by varying the microstructure from one material to another material with a specific gradient. Composite materials have greater advantages than the materials they are composed of. The plates are often subjected to in-plane forces due to components of aerodynamic or hydrodynamic forces acting on it. There are many studies on the free vibration of FGM plates, but vibration and buckling of FGM plates subjected to loading such as in turbines have not been studied much. Functionally graded materials have good thermal resistance and high stability in thermal conditions. Hence, the present work is to determine the buckling behavior of FGM plates subjected to in-plane varying loads.

2.3 OUTLINE OF THE PRESENT WORK

The present study deals with functionally graded material plates subjected to in plane loading and their behavior under the influence of different parameters like aspect ratio, side width ratio and gradient index and also different boundary conditions.

This thesis contains five chapters. A brief review is presented here.

In chapter 1, an introduction of functionally graded plates and applications of FGM plates is presented.

In chapter 2, the literature review pertaining to the previous work done in this area is detailed. An objective of the present study is also outlined in this chapter.

In chapter 3, a brief theory and formulation of finite element method is given. Methodology of buckling of FGM plates in ANSYS is explained in this chapter.

In chapter 4, detailed discussion about results of buckling of FGM plates by using ANSYS software is given. The plates are subjected to different in-plane loading and the effect of the different parameters like aspect ratio, side width ratio and gradient index on buckling load is presented.

In chapter 5, conclusions drawn from the studies are outlined.

CHAPTER 3

THEORY AND FORMULATION

3.1 GOVERNING DIFFERENTIAL EQUATION

A twisted FGM plate is shown in figure 3.1.

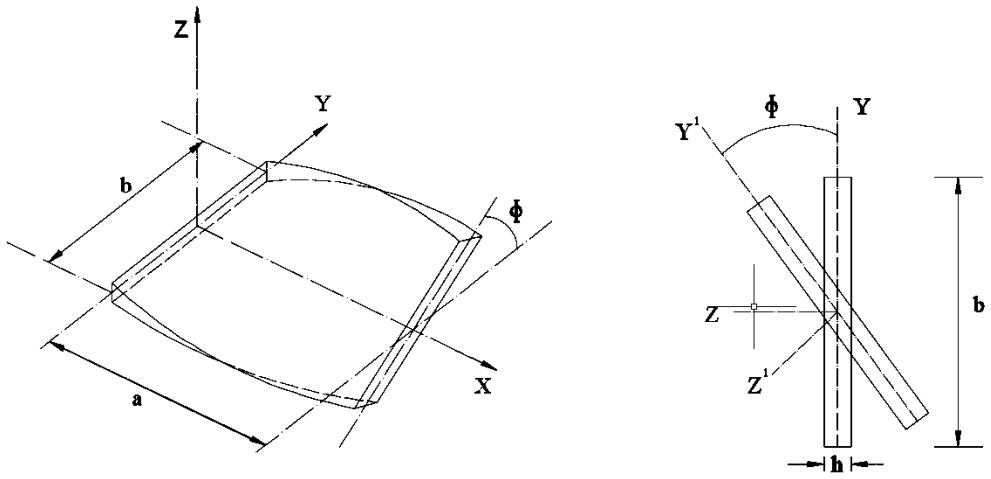

Figure 3.1: FGM twisted plate

In the figure 2.1, the dimensions 'a' and 'b' denote the length and width of the plate respectively and Φ is the angle of twist which in this case is zero as a flat plate is considered. 'h' is the thickness of the plate.

Figure 2.2 shows a differential element of the twisted panel. N_x ,N_y and N_{xy} are the internal axial forces, Q_x and Q_y are the shear forces and $M_x,\ M_y\ and\ M_{xy}$ are the moment resultants.

The differential equations of equilibrium for pretwisted doubly curved shell panel are given as:

(Chandrasekhara [3], Sahu and Datta [13])

$$\frac{\partial N_x}{\partial x} + \frac{\partial N_{xy}}{\partial y} - \frac{1}{2}\left(\frac{1}{R_y} - \frac{1}{R_x}\right)\frac{\partial M_{xy}}{\partial x} + \frac{Q_x}{R_x} + \frac{Q_y}{R_{xy}} = P_1\frac{\partial^2 u}{\partial t^2} + P_2\frac{\partial^2 \theta_x}{\partial t^2}$$

$$\frac{\partial N_{xy}}{\partial x} + \frac{\partial N_y}{\partial y} + \frac{1}{2}\left(\frac{1}{R_y} - \frac{1}{R_x}\right)\frac{\partial M_{xy}}{\partial x} + \frac{Q_x}{R_y} + \frac{Q_y}{R_{xy}} = P_1\frac{\partial^2 v}{\partial t^2} + P_2\frac{\partial^2 \theta_y}{\partial t^2}$$

$$\frac{\partial Q_x}{\partial x} + \frac{\partial Q_y}{\partial y} - \frac{N_x}{R_x} - \frac{N_y}{R_y} - 2\frac{N_{xy}}{R_{xy}} + {N_x}^0\frac{\partial^2 w}{\partial x^2} + {N_y}^0\frac{\partial^2 w}{\partial y^2} = P_1\frac{\partial^2 w}{\partial t^2} \quad (3.1)$$

$$\frac{\partial M_x}{\partial x} + \frac{\partial M_{xy}}{\partial y} - Q_x = P_3\frac{\partial^2 \theta_x}{\partial t^2} + P_2\frac{\partial^2 u}{\partial t^2}$$

$$\frac{\partial M_y}{\partial y} + \frac{\partial M_{xy}}{\partial x} - Q_y = P_3\frac{\partial^2 \theta_y}{\partial t^2} + P_2\frac{\partial^2 v}{\partial t^2}$$

Where,

${N_x}^0$ and ${N_y}^0$ are external in-plane forces in the x- and y- directions respectively.

R_x and R_y are the radii of curvature in the x- and y- directions respectively.

R_{xy} is the radius of twist.

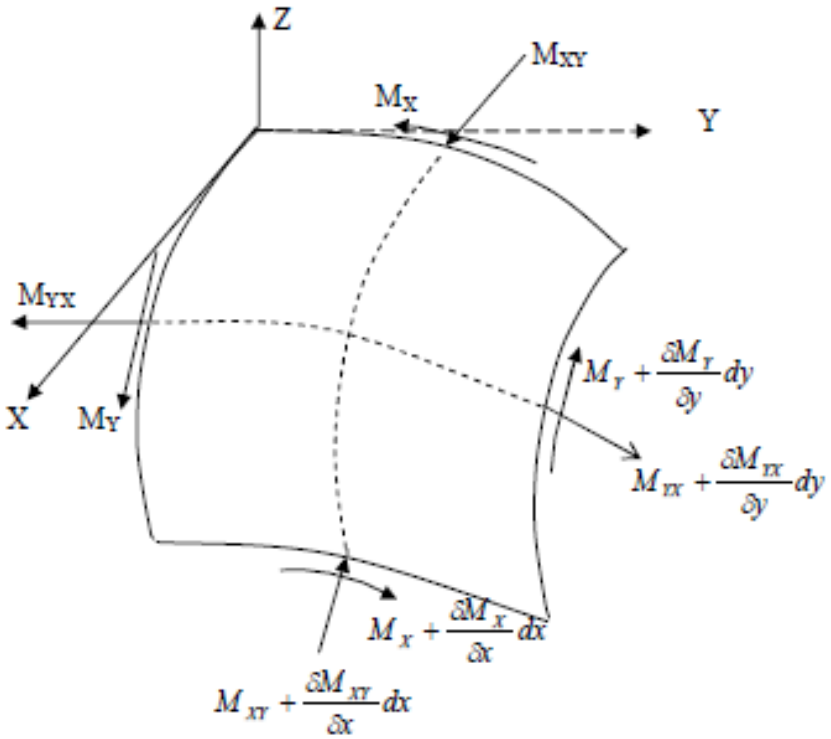

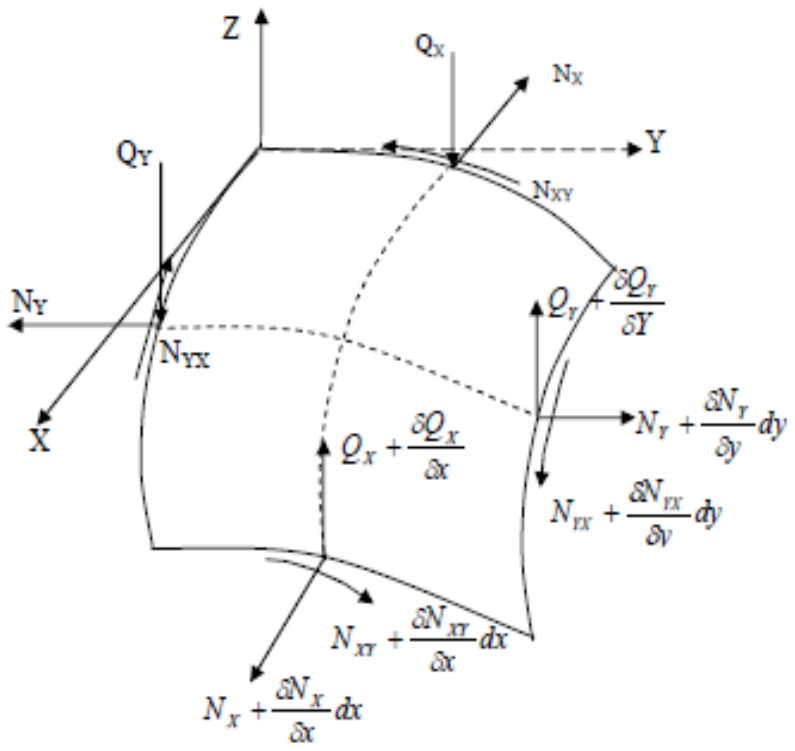

Figure 3.2: element of a shell panel

$$\left(P_1, P_2, P_3\right) = \sum_{k=1}^{n} \int_{z_{k-1}}^{z_k} (\rho)_k (1, z, z^2)\, \partial z \tag{3.2}$$

n = number of layers considered.

ρ_k = Density at k^{th} layer.

3.2 Constitutive Relations

The FGM plate taken for the study is made up of one side metal and the other ceramic. A parameter 'n' (material property index) shows the material variation along the thickness. The plate is fully ceramic for n = 0, and the plate is fully metal for n = α. Material properties are dependent on the n value and the position in the plate and vary according to the power law, (Reddy[11]), i.e.,

$$P_z = (P_t - P_b)V_f + P_b \tag{3.3}$$

$$V_f = \left(\frac{z}{h} + 0.5\right)^n \tag{3.4}$$

where P is the relevant material property, P_t and P_b are the material property at the top and bottom surfaces respectively and z is the location along the thickness measured from the mid-surface. V_f is the volume fraction index and n is the material property index. Young's modulus (E) varies according to the power law. Material density (ρ) and Poisson's ratio (μ) are assumed to be constant.

The material property of the FGM changes through the thickness. The numerical model is broken up into a number of layers in order to model the gradual change in properties of the FGM. Each layer is assumed to be isotropic. Material properties are calculated at the mid-point of each of these layers from the mid surface using power law, (Reddy [11]). Although the layered structure does not reflect the gradual change in material property, by using a sufficient number of layers the gradation can be approximated.

The linear constitutive relations are

$$\begin{Bmatrix} \sigma_x \\ \sigma_y \\ \tau_{xy} \\ \tau_{xz} \\ \tau_{yz} \end{Bmatrix} = \begin{bmatrix} Q_{11} & Q_{12} & 0 & 0 & 0 \\ Q_{12} & Q_{11} & 0 & 0 & 0 \\ 0 & 0 & Q_{44} & 0 & 0 \\ 0 & 0 & 0 & Q_{55} & 0 \\ 0 & 0 & 0 & 0 & Q_{66} \end{bmatrix} \begin{Bmatrix} \varepsilon_x \\ \varepsilon_y \\ \gamma_{xy} \\ \gamma_{xy} \\ \gamma_{xy} \end{Bmatrix}$$

where

$$Q_{11} = \frac{E}{(1-\nu^2)} \tag{3.5}$$

$$Q_{12} = \frac{\nu E}{(1-\nu^2)} \tag{3.6}$$

$$Q_{44} = Q_{55} = Q_{66} = \frac{E}{2(1+\nu)} \tag{3.7}$$

The constitutive relations for the FGM plate are given by:

$\{F\} = [D]\{\epsilon\}$

Where

$\{F\} = \{N_x \ N_y \ N_{xy} \ M_x \ M_y \ M_{xy} \ Q_x \ Q_y\}^T$

$\{\epsilon\} = \{\epsilon_x \ \epsilon_y \ \gamma_{xy} \ K_x \, K_y \ K_{xy} \ \varphi_x \ \varphi_y \}^T$

$$D = \begin{bmatrix} A_{11} & A_{12} & A_{16} & B_{11} & B_{12} & B_{16} & 0 & 0 \\ A_{21} & A_{22} & A_{26} & B_{21} & B_{22} & B_{26} & 0 & 0 \\ A_{16} & A_{22} & A_{66} & B_{16} & B_{22} & B_{66} & 0 & 0 \\ B_{11} & B_{12} & B_{16} & D_{11} & D_{12} & D_{16} & 0 & 0 \\ B_{21} & B_{22} & B_{26} & D_{21} & D_{22} & D_{26} & 0 & 0 \\ B_{16} & B_{22} & B_{66} & D_{16} & D_{22} & D_{66} & 0 & 0 \\ 0 & 0 & 0 & 0 & 0 & 0 & S_{44} & S_{45} \\ 0 & 0 & 0 & 0 & 0 & 0 & S_{45} & S_{55} \end{bmatrix} \tag{3.8}$$

Stiffness coefficients are defined as:

$\left(A_{ij}, B_{ij}, D_{ij}\right) = \sum_{k=1}^{n} \int_{z_{k-1}}^{z_k} \left[Q_{ij}\right]_k (1, z, z^2) dz$ for (i, j = 1, 2, 6)

$$S_{ij} = \kappa \sum_{k=1}^{n} \int_{z_{k-1}}^{z_k} \left[Q_{ij}\right]_k dz$$

A shear correction factor **κ** =5/6 is included in S_{ij} for numerical computations.

The forces and moment resultants are obtained as follows

$$\begin{bmatrix} N_x \\ N_y \\ N_{xy} \\ M_x \\ M_Y \\ M_{xY} \\ Q_x \\ Q_Y \end{bmatrix} = \int_{-h/2}^{h/2} \begin{Bmatrix} \sigma_x \\ \sigma_x \\ \tau_{xy} \\ \sigma_x z \\ \sigma_{yz} \\ \tau_{xy} z \\ \tau_{xz} \\ \tau_{yz} \end{Bmatrix} dz \tag{3.9}$$

Where σ_x, σ_y are the normal stresses along X and Y direction and τ_{xy},τ_{xz} and τ_{yz} are shear stresses in xy, xz and yz planes respectively.

3.3 Finite element formulation

Finite element software ANSYS 13.0 is used for the formulation of the FGM plate. SHELL 281 is used to model the element. SHELL 281 has eight nodes with six degrees of freedom per node: three translations in x-, y- and z- directions and three rotations. The first-order shear deformation theory is assumed for the modeling in ANSYS 13.0.

The plate is assumed to be made up of layers, where each layer is considered to be homogeneous and isotropic.

3.4 Strain Displacement Relations

Green-Lagrange's strain displacement relations are used. The elastic stiffness matrix is derived from the linear part of the strain and the geometric stiffness matrix from the nonlinear strain components. The linear strain displacement relations for a shell element are:

$$\xi_{xl}=\frac{\partial u}{\partial x}+\frac{w}{R_x}+zk_x$$

$$\xi_{yl}=\frac{\partial v}{\partial y}+\frac{w}{R_y}+zk_y$$

$$\gamma_{xyl}=\frac{\partial u}{\partial y}+\frac{\partial v}{\partial x}+\frac{2w}{R_{xy}}+zk_{xy} \tag{3.10}$$

$$\gamma_{xzl}=\frac{\partial w}{\partial x}+\theta_x-\frac{u}{R_x}-\frac{v}{R_{xy}}$$

$$\gamma_{yzl}=\frac{\partial w}{\partial y}+\theta_y-\frac{v}{R_y}-\frac{u}{R_{xy}}$$

Where the bending strains are

$$k_x=\frac{\partial \theta_x}{\partial x},\ k_y=\frac{\partial \theta_y}{\partial y}$$

$$k_{xy}=\frac{\partial \theta_x}{\partial y}+\frac{\partial \theta_y}{\partial x}+\frac{1}{2}\left(\frac{1}{R_y}-\frac{1}{R_x}\right)\left(\frac{\partial v}{\partial x}-\frac{\partial u}{\partial y}\right) \tag{3.11}$$

The linear strains are related to the displacements by the following relation

$$\{\varepsilon\} = [B]\{d_e\} \tag{3.12}$$

Where

$$\{d_e\} = \{u_1 v_1 w_1 \theta_{x1} \theta_{y1} \dots \dots \dots \dots \dots \dots . u_8 v_8 w_8 \theta_{x8} \theta_{y8}\} \tag{3.13}$$

$$[B] = [[B_1], [B_2] \dots \dots \dots \dots \dots \dots \dots . [B_8]] \tag{3.14}$$

The strain displacement matrix [B] is

$$[B_i] = \begin{bmatrix} N_{i,}x & 0 & \frac{N_i}{R_x} & 0 & 0 \\ 0 & N_{i,}y & \frac{N_i}{R_y} & 0 & 0 \\ N_{i,}y & N_{i,}x & 2\frac{N_i}{R_{xy}} & 0 & 0 \\ 0 & 0 & 0 & N_{i,}x & 0 \\ 0 & 0 & 0 & 0 & N_{i,}y \\ 0 & 0 & 0 & N_{i,}y & N_{i,}x \\ 0 & 0 & N_{i,}x & N_i & 0 \\ & & N_{i,}y & 0 & N_i \end{bmatrix} \tag{3.15}$$

3.5 Buckling

For stability problems, the stability equation can be expressed as the following eigenvalue problem:

$$([K] + \lambda[S])\{U\} = \{0\} \tag{3.16}$$

where matrix [K] denotes the stiffness matrix and matrix [S], the geometric stiffness matrix due to the in-plane stresses.

3.6 ANSYS methodology

Problems that can be solved in ANSYS include static/dynamic structure analysis (both linear and non-linear), heat transfer and fluid problems, as well as acoustic and electro-magnetic problems. There are three stages:

Preprocessing

This is to define the problem. The steps are

1. Define key points/lines/areas/volumes
2. Define element type and material/geometric properties
3. Meshing of lines or areas or volumes

Solution

Here loads and constraints are assigned and problem is solved.

Post-processing

This stage is to view and process the results like the list of nodal displacements, element forces and moments and deflection plots.

The present problem has been solved using ANSYS software. The FGM plate was first solved without loading in order to validate the methodology and the results compared to previous results for free vibration and buckling. Also the methodology was tested for a laminated composite plate with different types of edge loading and results compared to a result from a previous paper. The results matched closely in most cases. Then the software was run for studying the FGM plate with different types of in-plane loads.

CHAPTER 4

RESULTS AND DISCUSSIONS

4.1 Introduction

The FGM plate considered here consists of ceramic on top and metal at the bottom. In FGM plates, the material properties change continuously over the thickness by varying the gradient index (n). Those properties are density (ρ), Young's modulus (E) and also Poisson's (υ) ratio. If n = 0, then the plate is completely ceramic and if n = infinity then the plate is completely metal. Material properties depend on gradient index (n). By using the power law (Reddy[2000]) we can find out the material properties.

$$P(z) = (P_t - P_b)V + P_b \tag{4.1}$$

$$V_f = (z/h + ½)^n \tag{4.2}$$

Here P represents a material property like Young's modulus. P_t and P_b represents the relevant property at the top and bottom faces of the plate, h denotes the total thickness of the plate, n represents the gradient index or the material variation profile through thickness, V_f is the volume fraction and z is the thickness varyiation from the mid plane.

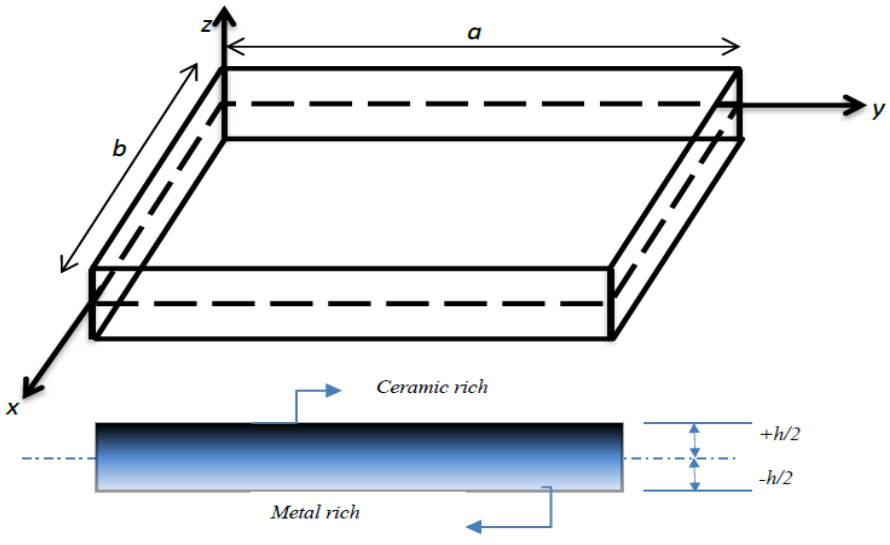

Figure 4.1: FGM plate

By using the MATLAB software, the Young's modulus of each layer was calculated. Poisson's ratio and density were kept constant. Then a model of FGM plate was developed by using ANSYS. Free vibration of cantilever FGM flat plate will be studied and results obtained and these results compared with previous results. Then the flat FGM plate is modeled and again results will be studied for plate with varying in plane loads.

Figure 4.1 shows the variation of V_f through the plate thickness.

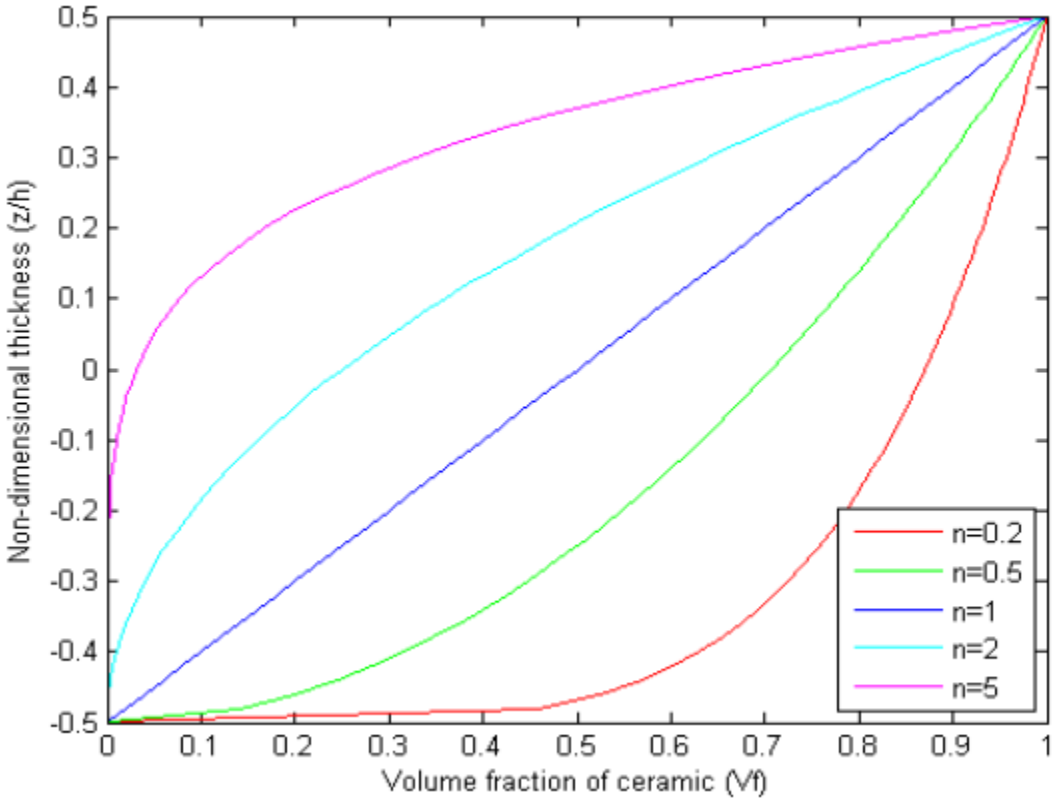

Figure 4.2: Variation of Volume fraction (V_f) through plate thickness

For n=1 the material properties changes linearly, n = 0 plate is total titanium and n= infinite plates is purely aluminum oxide

4.2 Results and discussions

The results of the free vibration analysis of functionally graded material cantilever plate (CFFF), simply supported plate (SSSS), and all edges clamped (CCCC) are presented. In ANSYS, an eight noded shell element SHELL 281 is used to model the FGM plate. This element has six degrees of freedom per node. As the material property of the FGM changes through the thickness, the numerical model is broken up into various layers in order to model the change in properties. Each layer is assumed to be isotropic. Material properties are calculated at the mid-point of each layer from the mid surface using power law. Although the layered structure does not reflect the actual gradual change in material property, by using a sufficient number of layers the gradation can be approximated. A convergence study was done to decide on the number of layers required to model accurately the FGM plate and mesh size for greater accuracy of results.

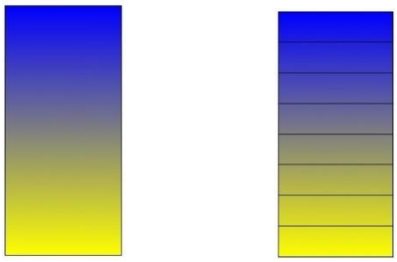

Figure 4.3: FGM section and equivalent laminated composite section

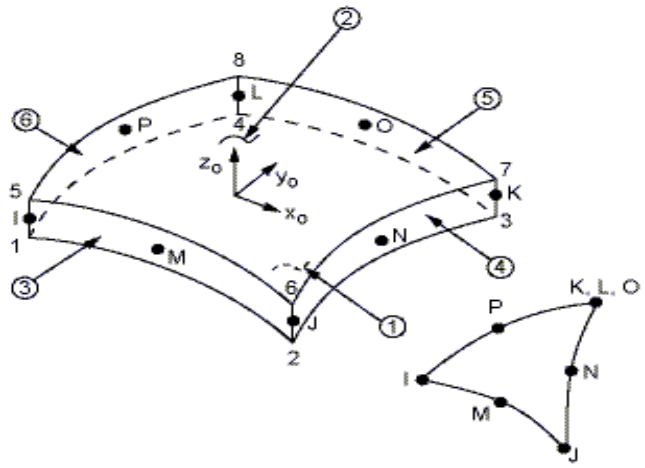

Figure 4.4: A SHELL 281 Element

4.2.1 Convergence study

For this study FGM plate consisting of aluminum oxide in a titanium (Al/Al_2O_3) matrix and square plate with aspect ratio a/b=1, b/h=100, (where a, b, and h are the width, length, and thickness) was taken. The properties of constituents are E_c =380GPa, $\vartheta = 0.3$, for aluminum oxide and E_m= 70GPa, $\vartheta = 0.3$, for Titanium.

The convergence study on simply supported flat FGM plate with gradient index n = 0 for different mesh divisions is shown in Table 4.1. The results show better convergence for 12×12 mesh division. The 12×12 mesh division is used for the further study.

The non-dimensional buckling load is given by $\bar{N} = N_{cr} \frac{a^2}{E_m h^3}$ [12]

Table 4.1: Convergence of non-dimensional buckling load (λ) of simply supported flat FGM plate (n = 0) with varying mesh size

a/b =1, b/h=100, n = 0

Mesh size	Buckling load (N_o) KN	Non-dimensional buckling load(λ)
4 × 4	696.59	19.90
6 6	687.00	19.63
8 × 8	686.60	19.62
10 × 10	686.53	19.61
12 × 12	686.52	19.61
	Reddy et al. [14]	19.57

The convergence study is done by using simply supported flat FGM plate with varying number of layers using gradient index n =1. The observations are given in Table 4.2. From the observations, it is concluded that 12 numbers of layers are sufficient to represent FGM property as an equivalent laminate section.

Table 4.2: Convergence of non- dimensional buckling load (λ) of simply supported flat FGM plate (n=1) with varying number of layers

a/b =1, b/h =100, n = 1

No of layers	Buckling load (N_o) KN	Non-dimensional buckling load(λ)
4	352.87	10.08
6	349.09	9.97
8	347.74	9.93
10	347.10	9.91
12	346.80	9.91
	Reddy et al. [14]	9.77

4.3 Buckling of FGM plate with in-plane loading

To validate the ANSYS formulation for in-plane loading, buckling of simply supported laminated composite plates with in-plane loading was first done. The results were compared with previous studies by Zhong and Gu [18]. The loading is given by the expression for compressive force

$$N_x = N_0(1 - \eta \frac{y}{b}) \quad (3.3)$$

Here η defines the linear variation of the in-plane load. The present discussion is confined to the case for $0 \leq \eta \leq 2$. For η = 0, it corresponds to the case of uniform compression. The pure in-plane bending comes about for η = 2. The non-dimensional critical load [22] is given by:

$$K = \frac{N_o b^2}{E_T h^3}$$

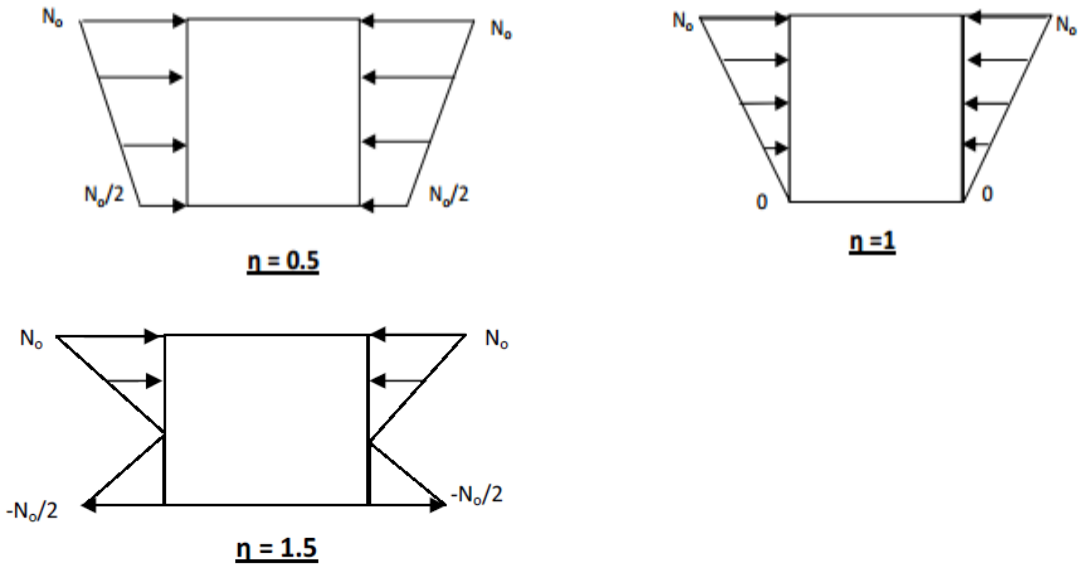

Figure 4.5: different load parameters [22]

The comparative study is done by using symmetric cross-ply laminated square plate $[0^0/90^0/0^0]$ subjected to various linearly varying loads as shown in figure 4.5.

Given properties of the laminated composite plate are [18]

$$\frac{E_L}{E_T} = 40, \quad \frac{G_{LT}}{E_T} = \frac{G_{LZ}}{E_T} = 0.6, \quad \frac{G_{ZT}}{E_T} = 0.5, \quad \vartheta = 0.25\,, \frac{h}{b} = 0.1$$

Table 4.3: Comparison of non-dimensional buckling load factors of symmetric cross-ply square plate with $\eta = 0, 0.5, 1$

	$\eta = 0$	$\eta = 0.5$	$\eta = 1$
Present study	21.698	28.70	40.268
Zhong and Gu [18]	22.317	29.432	40.999

The above table shows that the results are quite comparable with that of Zhong and Gu [18].

4.4 NUMERICAL RESULTS:-

As the formulation was validated in ANSYS, the effect of various parameters on the buckling of flat FGM plates with varying in-plane load was studied. Based on the convergence study, a mesh size of 12×12 and 12 number of layers was taken throughout the study. Table 4.4 shows the non-dimensional buckling load of flat FGM plates with different boundary conditions subject to linearly varying load by using different parameters like b/h ratio, aspect ratio(a/b) and gradient index(n).

Table 4.4: Variation of the non-dimensional buckling load $K = \frac{N_o b^2}{E_m h^3}$ with the load parameter "**η**" and b/h ratio for SSSS of square FGM plate (a/b =1), n= 1

Boundary condition	b/h ratio	Mode	η		
			0.5	1	1.5
SSSS	10	1	11.84	17.20	31.08
		2	17.48	24.78	39.91
	20	1	12.71	19.03	34.10
		2	19.39	27.59	44.69
	50	1	13.14	19.69	35.44
		2	20.17	28.75	46.72
	100	1	13.27	19.87	35.79
		2	20.35	29.00	47.20
	200	1	13.32	19.94	35.94
		2	20.42	29.12	47.41
	250	1	13.32	19.96	35.96
		2	20.43	29.14	47.44

It is observed from Table 4.4 that for the simply supported plate, as the b/h ratio increases, the buckling load increases till about b/h= 200.

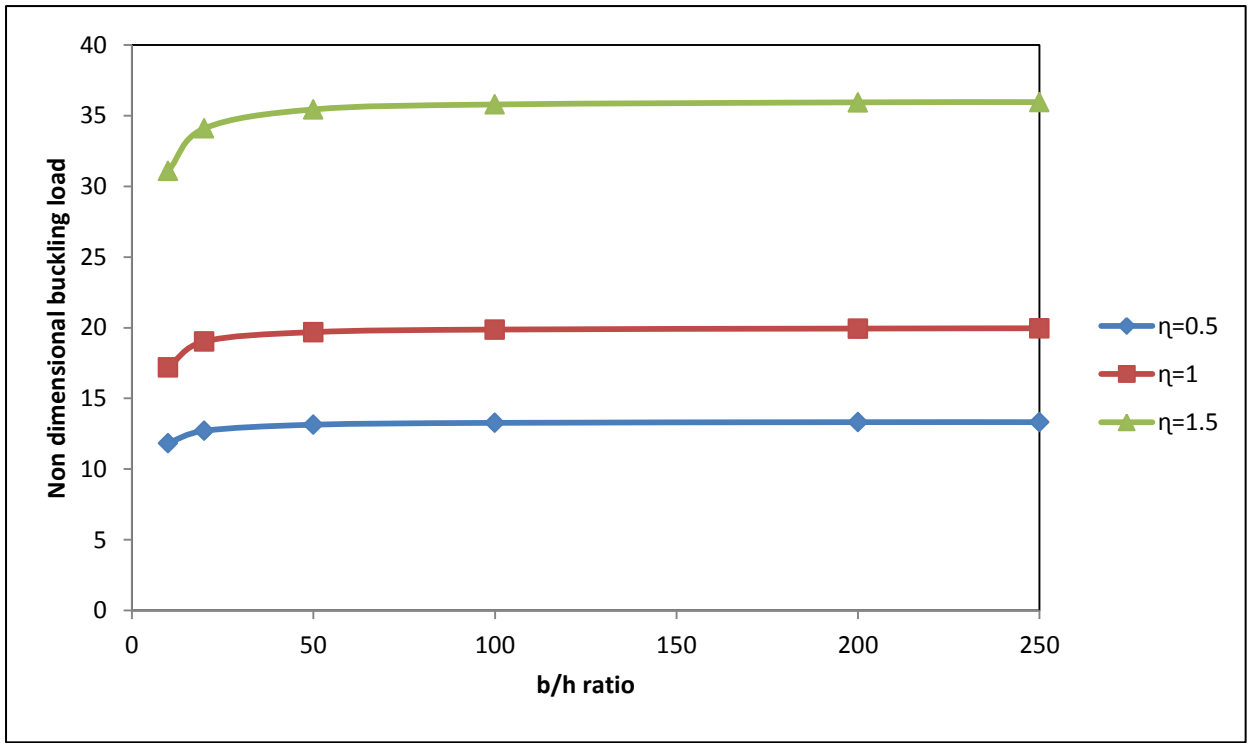

Figure 4.6: Variation of non-dimensional buckling load with b/h ratio and load parameter (η) for SSSS plate and a/b =1

Variation of the buckling load with aspect ratio for a simply supported plate with various loading conditions is shown in Table 4.5. The buckling load is found to decrease as the aspect ratio increases.

In Table 4.6, a plate with all edges simply supported is analysed for varying gradient index. It is observed here that as the gradient index increases, the buckling load decreases for all types of varying load.

Table 4.5: Variation of the non-dimensional buckling load $K = \frac{N_o b^2}{E_m h^3}$ with the load parameter "**η**" and aspect ratio (a/b) ratio for SSSS of FGM plate, n = 1

Boundary condition	Aspect ratio(a/b)	mode	η		
			0.5	1	1.5
SSSS	0.5	1	20.39	28.62	42.53
		2	53.53	72.18	90.71
	1	1	13.32	19.96	35.96
		2	20.42	29.14	47.44
	2	1	13.24	19.60	33.30
		2	15.47	22.92	43.39
	3	1	13.27	19.72	33.94
		2	14.51	21.53	42.42

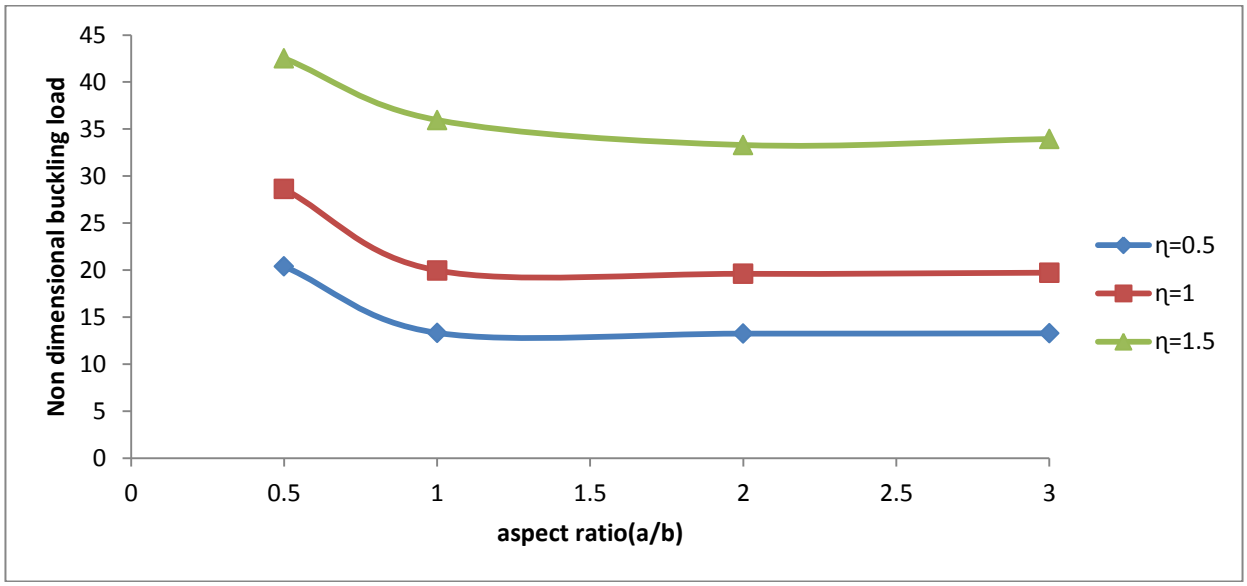

Figure 4.7: Variation of non-dimensional buckling load with aspect ratio (a/b) and load parameter (η) for SSSS plate and b/h =250

Table 4.6: Variation of the non-dimensional buckling load $K = \frac{N_o b^2}{E_m h^3}$ with the load parameter "**η**" and gradient index (n) for SSSS of FGM plate , aspect ratio (a/b)=1, b/h=250.

Boundary condition	Gradient index (n)	mode	η		
			0.5	1	1.5
SSSS	0	1	26.16	39.24	71.19
		2	40.31	57.32	92.86
	0.5	1	16.85	25.25	45.68
		2	25.90	36.88	59.88
	1	1	13.32	19.60	35.96
		2	20.43	22.92	47.44
	5	1	8.87	13.20	23.71
		2	13.50	19.27	31.44
	10	1	8.24	11.99	22.23
		2	12.64	17.49	29.34
	50	1	8.075	12.10	21.77
		2	12.38	17.65	28.76
	100	1	8.14	10.12	21.91
		2	12.47	14.78	29.03

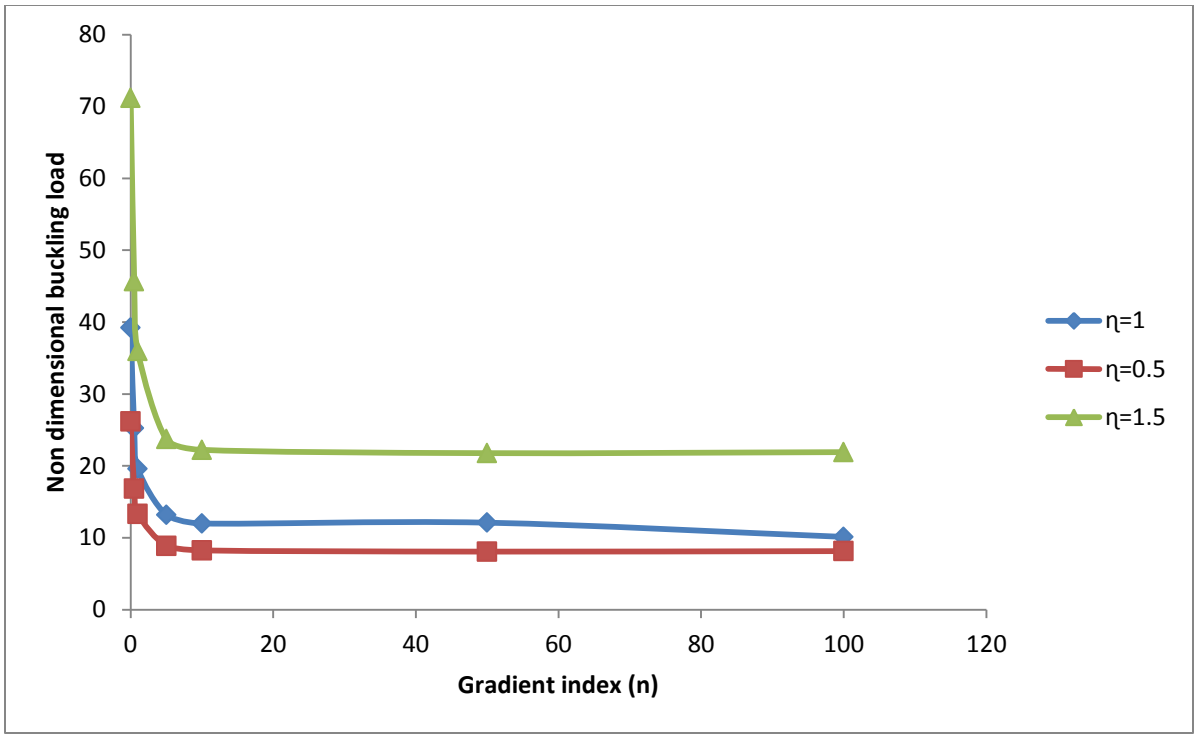

Figure 4.8: Variation of Non dimensional buckling with gradient index (n) and load parameter (η) for SSSS plate and b/h=250

The next study was done for a plate with all edges clamped **(CCCC)** and is presented in Table 4.7.

Table 4.7:-Variation of the non-dimensional buckling load $K = \frac{N_o b^2}{E_m h^3}$ with the load parameter "**η**" and b/h ratio for CCCC of FGM plate

Boundary condition	b/h ratio	mode	η		
			0.5	1	1.5
CCCC	10	1	45.712	66.64	109.32
		2	54.20	77.19	114.97
	20	1	53.36	78.54	139.59
		2	66.64	96.54	155.81
	50	1	55.93	82.46	148.96
		2	70.97	103.15	169.18
	100	1	56.37	83.14	150.62
		2	71.69	104.31	171.71
	200	1	56.68	83.629	151.88
		2	72.09	105.02	173.85
	250	1	56.84	83.875	152.50
		2	72.272	105.36	174.92

Here too, the buckling load is found to increase as the b/h ratio increases. A similar behavior is observed for a cantilever plate with changing b/h ratio as seen in **Table 4.8**.

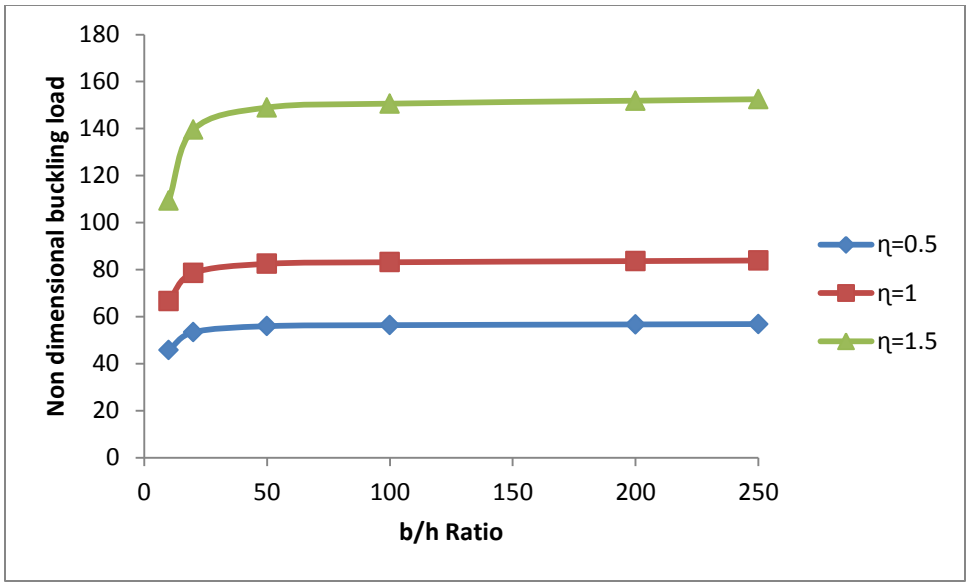

Fig 4.9: Variation of non-dimensional buckling load with b/h ratio and load parameter (η) for CCCC plate and a/b =1

Table 4.8: Variation of the non-dimensional buckling load $K = \frac{N_o b^2}{E_m h^3}$ with the load parameter "**η**" and b/h ratio for CFFF of square FGM plate (a/b=1)

Boundary condition	b/h ratio	Mode	η		
			0.5	1	1.5
CFFF	10	1	0.773	1.108	1.722
		2	5.625	7.67	8.955
	20	1	0.779	1.119	1.753
		2	5.449	8.0592	9.455
	50	1	0.781	1.125	1.769
		2	6.126	8.2014	9.649
	100	1	0.7822	1.125	1.773
		2	6.171	8.232	9.636
	200	1	0.783	1.127	1.776
		2	6.209	8.246	9.714
	250	1	0.783	1.127	1.776
		2	6.215	8.248	9.718

For a plate with all edges clamped, the buckling load for all types of in-plane loading is found to initially decrease with increasing aspect ratio upto an aspect ratio of 2 and then increase as seen in Table 4.9. This is also shown in figure 4.10.

Table 4.9: Variation of the non-dimensional buckling load $K = \frac{N_o b^2}{E_m h^3}$ with the load parameter "**η**" and aspect ratio (a/b) ratio for CCCC of FGM plate, n = 1, b/h=250

Boundary condition	Aspect ratio(a/b)	mode	η		
			0.5	1	1.5
CCCC	0.5	1	70.11	100.69	160.74
		2	118.9	169.498	248.78
	1	1	56.84	83.875	152.50
		2	72.27	105.36	174.92
	2	1	65.34	96.72	33.30
		2	86.63	127.16	43.39
	3	1	81.59	119.8	33.94
		2	99.03	145.38	42.42

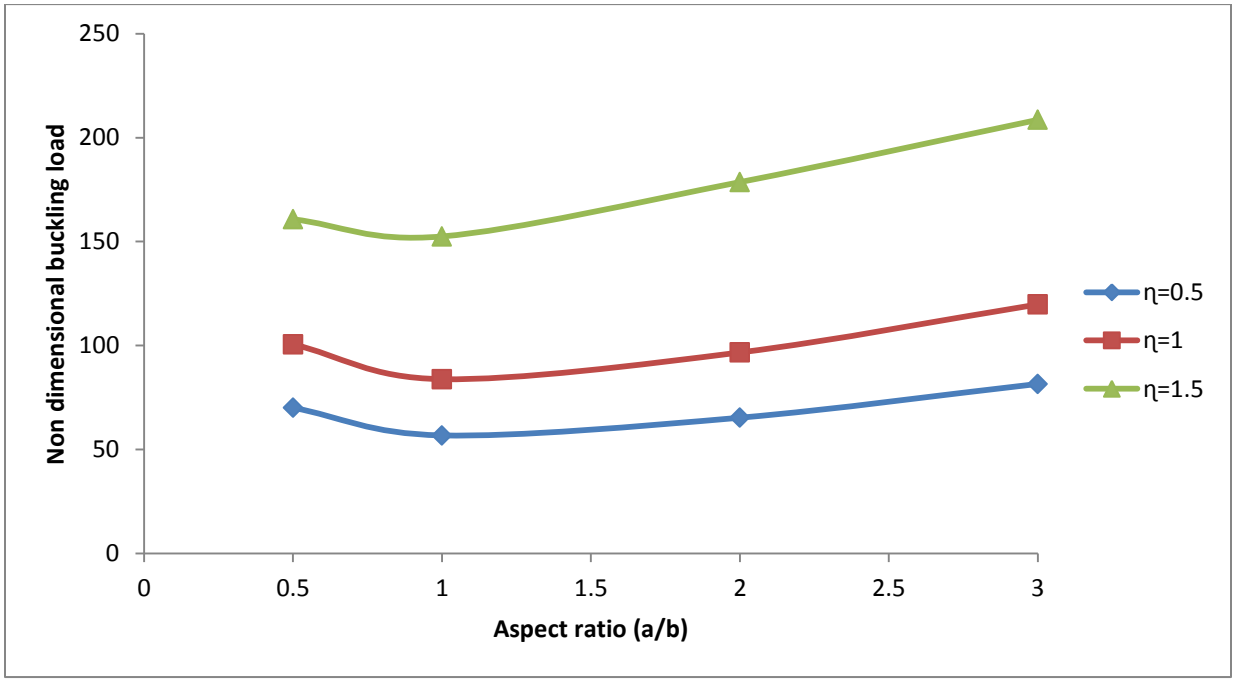

Figure 4.10: Variation of Non dimensional buckling with aspect ratio (a/b) and load parameter (η) for CCCC plate

Table 4.10 shows the effect of the variation in gradient index on the buckling load for a plate with all edges clamped. As the gradient index increases, the buckling load decreases.

Table 4.10: Variation of the non-dimensional buckling load $K = \frac{N_o b^2}{E_m h^3}$ with the load parameter "**η**" and gradient index (n) for CCCC FGM plate , aspect ratio (a/b) =1, b/h = 250.

Boundary condition	Gradient index (n)	mode	η		
			0.5	1	1.5
CCCC	0	1	113.60	167.61	304.63
		2	144.46	210.54	349.12
	0.5	1	72.60	107.13	194.78
		2	92.32	134.58	223.40
	1	1	56.84	83.88	152.50
		2	72.27	105.36	174.92
	5	1	37.24	54.94	99.79
		2	47.36	69.00	114.25
	10	1	35.05	51.71	93.91
		2	44.58	64.94	107.48
	50	1	34.29	50.59	91.86
		2	43.61	63.53	105.12
	100	1	34.43	50.81	92.29
		2	43.81	63.82	105.65

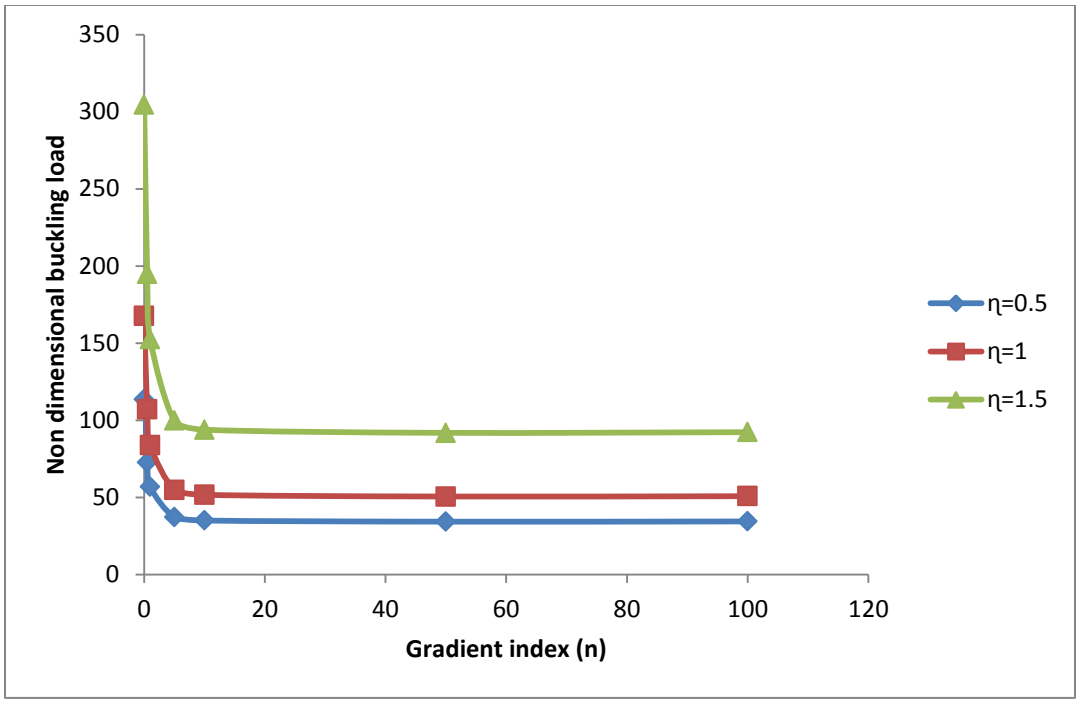

Figure 4.11: Variation of non-dimensional buckling load with gradient index (n) and load parameter (η) for CCCC plate and a/b=1

The study is now extended to cantilever plates. Table 4.11 shows the effect of increasing aspect ratio. As the aspect ratio increases, the buckling load decreases consistently.

Table 4.11: Variation of the non-dimensional buckling load $K = \frac{N_o b^2}{E_m h^3}$ with the load parameter "**η**" and aspect ratio (a/b) ratio for cantilever FGM plate

Boundary condition	Aspect ratio(a/b)	mode	η	
			0.5	1
CFFF	0.5	1	3.13	4.12
		2	8.42	17.11
	1	1	0.400	0.576
		2	3.182	4.223
	2	1	0.193	0.286
		2	1.72	2.379
	3	1	0.085	0.126
		2	0.76	1.100

Figure 4.12 shows the variation of buckling load with b/h ratio for a cantilever plate. There appears to be almost no effect on the buckling load as the b/h ratio increases.

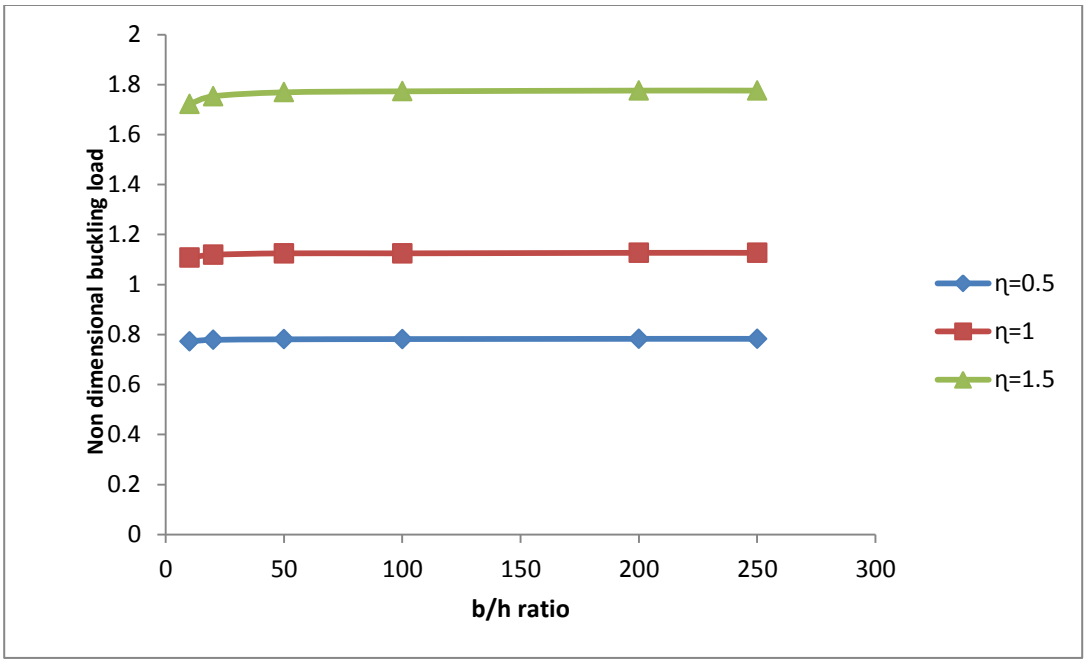

Fig 4.12: Variation of non-dimensional buckling load with b/h ratio and load parameter (η) for a square cantilever plate

Table 4.12 shows that as the gradient index of the cantilever FGM plate is increased, the buckling load decreases. For n = 10 onwards, the buckling load remains constant for all types of in-plane loading. This is also shown in figure 4.13.

Table 4.12: Variation of the non-dimensional buckling load $K = \frac{N_o b^2}{E_m h^3}$ with the load parameter "**η**" and gradient index (n) for square cantilever FGM plate , aspect ratio (a/b) =1, b/h =250.

Boundary condition	Gradient index (n)	mode	η		
			0.5	1	1.5
CFFF	0	1	1.57	2.25	3.55
		2	12.43	16.50	19.44
	0.5	1	1.00	1.44	2.27
		2	7.94	10.54	12.41
	1	1	0.783	1.126	1.776
		2	6.215	8.248	9.718
	5	1	0.514	0.74	1.166
		2	4.079	5.42	6.38
	10	1	0.48	0.696	1.098
		2	3.84	5.099	6.007
	50	1	0.47	0.68	1.07
		2	3.76	4.99	5.88
	100	1	0.47	0.68	1.08
		2	3.77	5.01	5.90

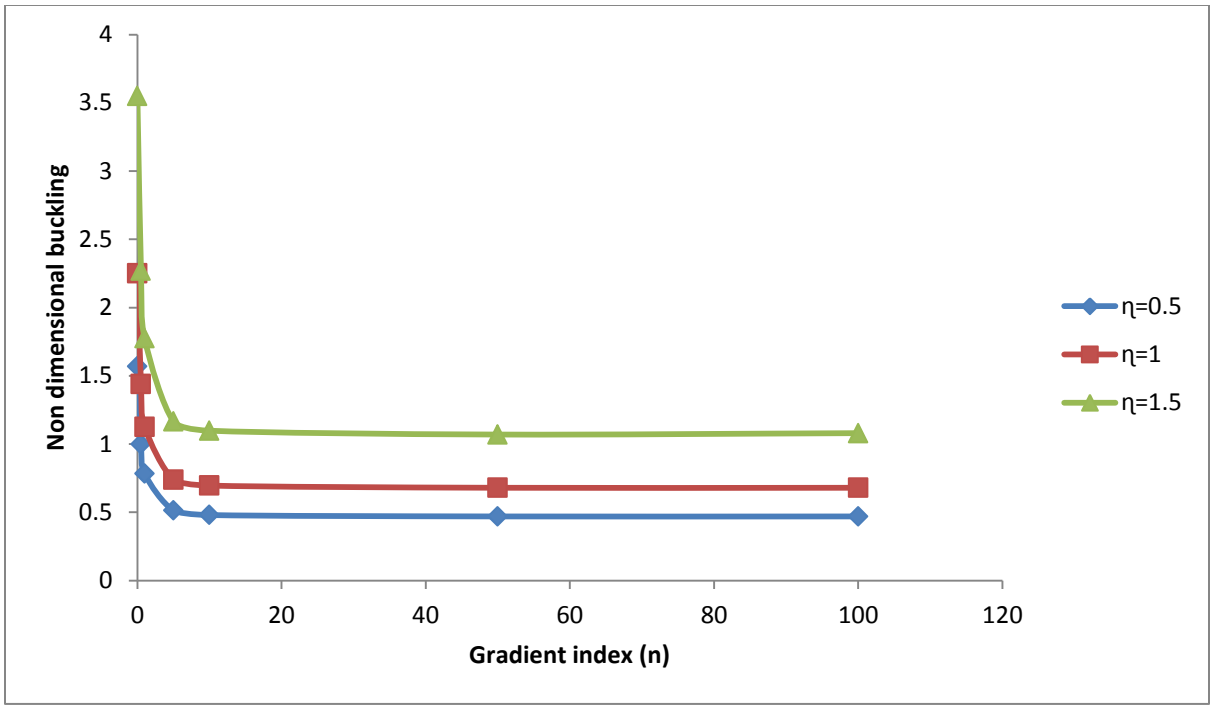

Fig 4.13: Variation of non-dimensional buckling load with gradient index (n) and load parameter (η) for square cantilever plate.

The effect of increasing aspect ratio for all the different plates with different boundary conditions on the buckling load for uniformly varying load (η =1) is shown in Figure 4.14. Similar behavior is observed for the simply supported plate and cantilever plate while the plate with all edges clamped shows an increase in buckling load as the aspect ratio increases beyond 2.

Again with increasing b/h ratio, the simply supported plate and cantilever plate behave similarly while the plate with all edges clamped shows a marked increase in buckling load at b/h = 50.

For the cantilever plate, the increase in gradient index has no effect on the buckling load value for a uniformly varying load. The simply supported plate and the clamped plate show a decrease upto n = 10 and then remain constant too.

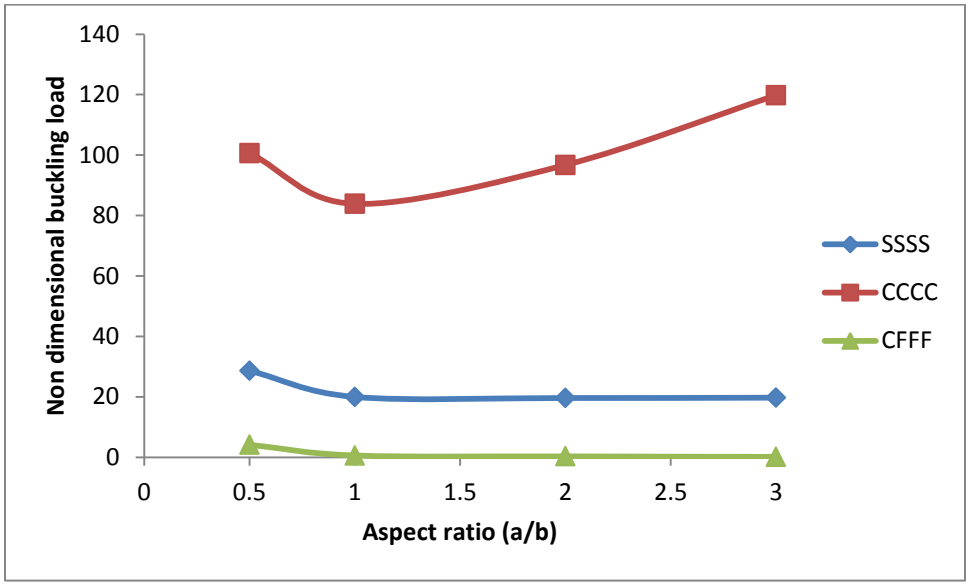

Figure 4.14: Variation of non-dimensional buckling load with aspect ratio (a/b) for FGM plates with different boundary conditions for load parameter (η =1).

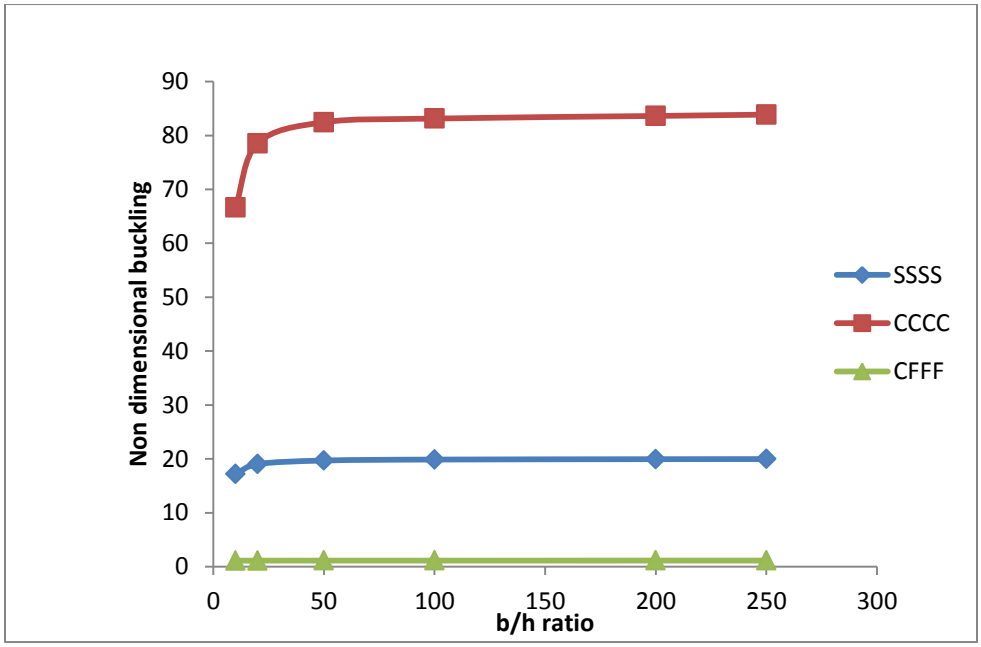

Figure 4.15: Variation of non-dimensional buckling load with b/h ratio for FGM plates with different boundary conditions for load parameter (η =1).

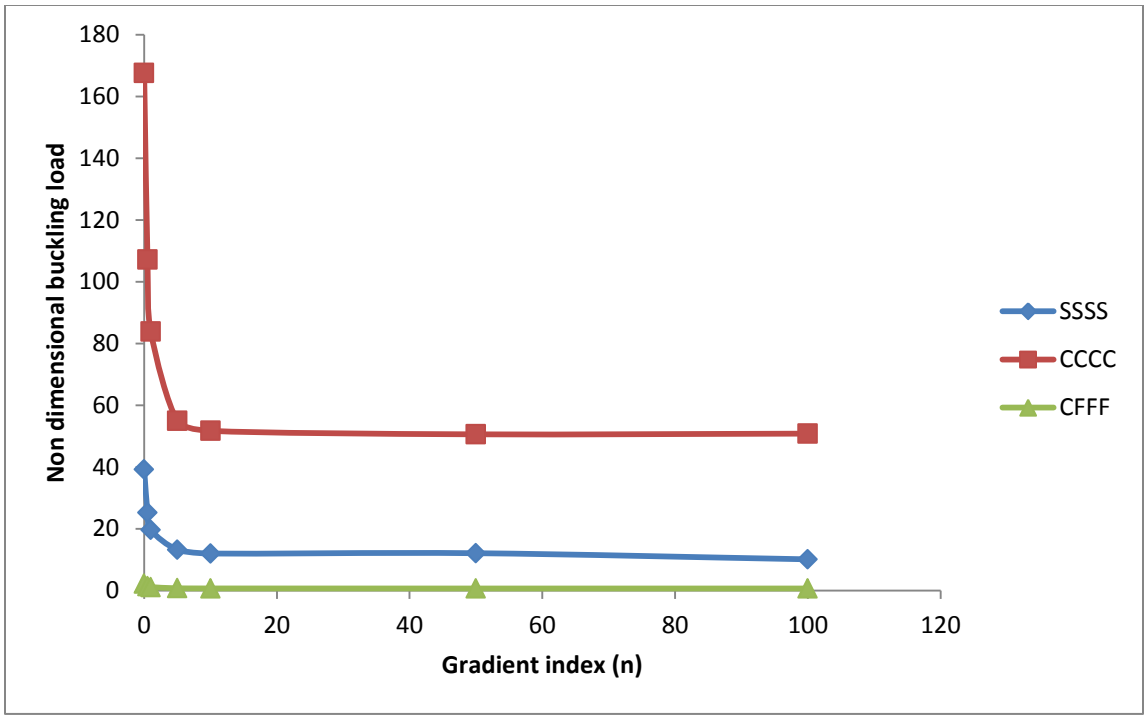

Figure 4.16: Variation of non-dimensional buckling load with gradient index n for FGM plates with different boundary conditions for load parameter (η =1).

CHAPTER 5
CONCLUSIONS

The behavior of buckling of functionally graded material (FGM) plate subjected to various types of in-plane loading was studied. The work has been done in ANSYS. The effects of geometrical parameters like side width ratio, aspect ratio (a/b), gradient index and different boundary conditions on buckling parameters of FGM plates has been studied.

From the above study, it is observed that for all boundary conditions, with increasing side width ratio, non-dimensional buckling load increases.

Also for simply supported and cantilever plates, while increasing the aspect ratio and gradient index, the non-dimensional buckling load decreases. In fact for cantilever plates, there seems to be no effect of increase in gradient index for all loading types beyond n =10.

But in plate with all edges clamped, non-dimensional buckling load decreases up to a/b=1 and with further increase in aspect ratio, the buckling load parameter increases.

The loading with $\eta = 1.5$ gives highest buckling load value as compared to the trapezoidal loading ($\eta = 0.5$) and uniformly varying load ($\eta = 1$).

Based on above conclusions, the FGM plate may be suitably designed for different loading types so that buckling load may be optimized.

Scope for the future work

In this paper, the behavior of buckling of FGM plates with in-plane loading with different boundary conditions was studied. In this study, ceramic and metal were assumed as FGM material. The study may be extended to different material of FGM and their buckling behavior while applying in-plane loading with different boundary conditions may be studied.

The thermal buckling of FGM plates with different boundary conditions subjected to in-plane loading and the effect of different parameters like aspect ratio, side depth ratio and gradient index may also be investigated further.

REFERENCES

[1] Abrate, S. (2006): Free vibration, buckling, and static deflections of functionally graded plates, *Composites Science and Technology*, 66, pp. 2383–2394

[2] Alinia, M. M., Soltanieh, G., &Amani, M. (2012). Inelastic buckling behavior of stocky plates under interactive shear and in-plane bending. *Thin-Walled Structures*, *55*, 76-84

[3] Chandrashekhara, K. (1989)**:** Free vibrations of anisotropic laminated doubly curved shells, *Computers and Structures*, Vol.**33** (2), pp.435-440

[4]Chung YL, Chi SH., (2001): The residual stress of functionally graded materials. *Journal of the Chinese Institute of Civil and Hydraulic Engineering*, 13, pp 1–9.

[5] Ebrahimi and Rastgo(2008): Free Vibration Analysis of Smart FGM Plates, *World Academy of Science, Engineering and Technology*,2, pp.01-29.

[6] Hadi, A.R., Daneshmehr, S.M., Nowruzpour M., Hosseini, M. and Ehsani, F.(2013): Elastic analysis of functionally graded Timoshenko beam subjected to transverse loading, *Technical Journal of Engineering and Applied Sciences*., 3, pp.1246-1254

[7] Javaheri R, Eslami MR., (2002): Buckling of functionally graded plates under inplane compressive loading, ZAMM, 82(4), pp 277–83.

[8] Kang, J.H., Leissa AW., (2005), Exact solutions for the buckling of rectangular plates having linearly varying in-plane loading on two opposite simply supported edges, Int Journal of Solids and Structures, 42, pp 4220–4238.

[9]Lanhe W.,(2004): Thermal buckling of a simply supported moderately thick rectangular FGM plate, *Composite structures*, 64, pp 211–8.

[10] Praveen, G.N., and Reddy, J.N. (1998): Nonlinear transient thermo elastic analysis of functionally graded ceramic-metal plates, *International Journal of Solids and Structures*, 35, pp. 4457-4476.

[11] Reddy, J.N. (2000): Analysis of functionally graded plates, *International Journal for Numerical methods in engineering*, 47, pp. 663–684.

[12] Saha, R., Maiti, P.R. (2012): Buckling of simply supported FGM plates under uniaxial load, *Internatioanl Journal of Civil and Structural Engineering*, Vol.2, No.4

[13]Sahu, S.K., and Datta, P.K. (2003): Dynamic stability of laminated composite curved panels with cutouts, *Journal of Engineering Mechanics*, ASCE, **129**(11), pp.1245-1253.

[14] Sidda Reddy, Suresh Kumar. J, Eswara Reddy. C and Vijaya Kumar Reddy. K,(2013) Buckling Analysis of Functionally Graded Material Plates Using Higher Order Shear Deformation Theory, *Journal of Composites*, Volume 2013, Article ID 808764, 12 pages.

[15] Yang,J., Kitipornchai,S., and Liew,K.M.(2001):Semi-analytical solution for nonlinear vibration of laminated FGM plates with geometric imperfections, *International Journal of Solids and Structures*, 41, pp.2235-2257.

[16] Yang, J., and Shen, H.S. (2002, 2003): Vibration characteristic and transient response of shear deformable functionally graded plates in thermal environments, *Journal of Sound and Vibration*,255, pp.579–602.

[17] Wattanasakulpong, N., Ungbhakorn, V.(2012):Thermal buckling and elastic vibration of third order shear deformable functionally graded beams, *International Journal of Mechanical Science*, 53, pp. 734-743.

[18] Zhong, H., Gu, C. (2007): Buckling of symmetrical cross-ply composite rectangular plates under a linearly varying in-plane load, *Composite Structures*, 80, pp.42–48.